A Comparison of In Vivo ^{13}C MR Brain Glycogen Quantification at 9.4 and 14.1 T

Ruud B. van Heeswijk,[1]* Yves Pilloud,[1] Florence D. Morgenthaler,[1] and Rolf Gruetter[1–3]

The high molecular weight and low concentration of brain glycogen render its noninvasive quantification challenging. Therefore, the precision increase of the quantification by localized ^{13}C MR at 9.4 to 14.1 T was investigated. Signal-to-noise ratio increased by 66%, slightly offset by a T_1 increase of 332 ± 15 to 521 ± 34 ms. Isotopic enrichment after long-term ^{13}C administration was comparable (~40%) as was the nominal linewidth of glycogen C1 (~50 Hz). Among the factors that contributed to the 66% observed increase in signal-to-noise ratio, the T_1 relaxation time impacted the effective signal-to-noise ratio by only 10% at a repetition time = 1 s. The signal-to-noise ratio increase together with the larger spectral dispersion at 14.1 T resulted in a better defined baseline, which allowed for more accurate fitting. Quantified glycogen concentrations were 5.8 ± 0.9 mM at 9.4 T and 6.0 ± 0.4 mM at 14.1 T; the decreased standard deviation demonstrates the compounded effect of increased magnetization and improved baseline on the precision of glycogen quantification. Magn Reson Med 000:000–000, 2011. © 2011 Wiley Periodicals, Inc.

Key words: brain glycogen; concentration quantification; C13 spectroscopy; 14.1 T; T_1 relaxation

INTRODUCTION

Glycogen (Glyc) is a branched polysaccharide chain of glucosyl units and the main form of energy storage in the brain (1). Glycogen has much lower concentrations in the brain than in tissues such as the liver and muscles (on the order of 5 mM vs. >100 mM in the liver) (2), which until recently caused its importance as a cerebral energy store to be largely neglected. Furthermore, besides brain energy homeostasis, brain glycogen has been linked to memory formation (3) and neurotransmitter synthesis (4), while its turnover has also been shown to change under physiological changes such as mild sleep deprivation (5) and lithium treatment (6). Therefore, the precise metabolic role of brain glycogen remains to be fully elucidated (1).

To date, ^{13}C localized nuclear magnetic resonance (NMR) in combination with ^{13}C label incorporation through a substrate such as [1-^{13}C] glucose (Glc) (7) is the only method to study brain glycogen metabolism noninvasively in vivo. Several ^{13}C NMR methods have been proposed to quantify its concentration (8–10), but these remain challenging and time consuming, not only due to the low amount of signal per unit of time caused by the carbon nucleus and glycogen concentration but also due to its polysaccharide structure. This latter challenge expresses itself as short T_1 and T_2 relaxation times (on the order of a few hundred and 5–10 ms, respectively; Ref. 11), caused by long correlation times. The Glyc C1 resonance is located next to those of Glc C1β and C1α (100.5, 96.6, and 92.7 ppm, respectively), which makes the three resonances straightforward to detect at the same time, but which may hamper their peak fitting.

All of the above limitations (low relative signal, broad linewidth, and short relaxation times) change with magnetic field strength; an increase in magnetic field strength might thus have a compounded beneficial effect on the complicated quantification process. Therefore, the aim of this study was to estimate the potential improvements in the quantification of the Glyc C1 resonance when the magnetic field strength B_0 was increased from 9.4 to 14.1 T.

MATERIALS AND METHODS

To quantify brain glycogen, ^{13}C localized NMR spectroscopy was performed using two horizontal bore animal MR scanners (Agilent Technologies, Santa Clara, CA): an actively shielded 9.4 T/31 cm magnet and a 14.1 T/26 cm magnet. Both magnets were equipped with 12-cm inner-diameter gradient sets that allowed a maximum gradient strength of 400 mT/m in 120 μs. All experimental conditions for glycogen quantification in the two MR scanners were identical, except when specified otherwise.

In both magnets, a 14-mm quadrature ^{1}H coil with a single three-loop 10-mm diameter ^{13}C coil (12) was used for transmission and reception. As the signal-to-noise ratio (SNR) of a coil is proportional to the square root of its quality (Q)-factor: SNR $\sim Q^{0.5}$ (13), the loaded Q factors of these coils were determined on a network analyzer (Agilent Technologies); loading the coil was done by placing it on top of a 50-mL tube filled with 500 mM NaCl. The Q factor was then approximated as its resonance frequency divided by the full width at half maximum of the tuned and matched resonance (i.e., $f_0/\Delta f$) detected by a sniffer loop. Noise figures for the receive chains of both scanners were also obtained with a noise diode (Micronetics, Hudson, NH).

All animal experiments were conducted according to local guidelines after obtaining approval from the local

animal ethical committee. Male Sprague–Dawley rats (∼220 g, $n = 4$ at 9.4 T, $n = 3$ at 14.1 T, Charles River Laboratories, L'Arbresle, France) were prelabeled at the Glyc C1 position as previously described (9), such that the Glyc C1 isotopic enrichment (IE) was high (∼40%) and constant. Briefly, two evenings before the experiments, rats were fasted overnight to minimize endogenous unlabeled liver Glyc stores. The following morning, 24 h before the experiments, the rats were given 10% w/v [1-^{13}C] Glc (IE = 99%, Cambridge Isotope Laboratories, Andover, MA) in tap water solution ad libitum as their only source of food and water, which would allow the glycogen IE to reach an empirically established steady state of 35–45% (9).

Before placing the animals in the magnet, they were anesthetized with isoflurane (5% for induction and 1.8–2.0% for maintenance) in a 70:30 mixture of nitrous oxide and oxygen. After intubation and initialization of assisted breathing, a femoral artery was catheterized for blood sampling and a femoral vein was catheterized for infusion of α-chloralose (Acros Organics, Geel, Belgium) and 20% w/v [1-^{13}C] Glc in saline. This Glc infusion was initially set at 40% IE through mixing of 99% [1-^{13}C] Glc with nonlabeled Glc to reflect the previously mentioned steady state Glyc IE. The infusion rate was approximately ∼0.2 mg Glc/h to maintain constant euglycemia. After surgery, isoflurane was turned off and replaced by α-chloralose alone (26.7 mg/kg/h). Blood samples were taken every 30 min for blood gas and glucose analysis, which were used for according adjustments of the respiration volume and frequency ($pCO_2 = 39 \pm 2$ mmHg, $pO_2 > 100$ mmHg, pH = 7.41 ± 0.03, [blood Glc] = 7 ± 1 mM). Temperature and breathing were monitored through a rectal probe and respiration pillow, respectively. A silicon tube with circulating warm water was placed on the body of the animal to maintain constant body temperature ($T = 37.7 \pm 0.2°C$) through a feedback loop. The radiofrequency coil was then carefully positioned such that it just touched the top of the rat head (i.e., <0.5 mm distance from the top of the head for the entire ^{13}C loop) to optimize the use of the sensitive volume of the coil. The animal was then inserted into the MR scanner.

After FASTMAP (14) shimming (resulting in a 22 and 26 Hz water linewidth at 9.4 and 14.1 T, respectively, for a large 6 × 8 × 10 mm^3 voxel in the brain), the IE of N-acetyl aspartate (NAA) was determined with a carbon-edited ^{1}H STEAM sequence, which was used to calculate the IE of brain Glyc C1 as described previously (9). In short, this sequence uses a ^{13}C inversion pulse in the middle STEAM period to invert the ^{13}C-coupled NAA C6 resonances every other acquisition through their J-coupling, which through subtraction edits for the ^{13}C-coupled resonances to determine the ^{13}C-NAA/[NAA] ratio. Previous studies (9) have shown that under these experimental conditions the in vivo Glyc C1 IE is ∼2.2 times this NAA IE under these experimental conditions. To keep the Glyc enrichment percentage constant, the IE of the Glc infusion was changed accordingly.

Localized ^{13}C spectroscopy was performed on a 6 × 8 × 10 mm^3 voxel with a modified SIRENE pulse sequence (15), which consisted of 3D outer volume suppression, 1D inversion nulling, and an added 1D Image-Selected

In vivo Spectroscopy (ISIS) module (16). Bilevel Waltz-16 nuclear Overhauser effect (NOE) and decoupling were applied at the Glyc/Glc ^{1}H frequency. The SNR of this volume was determined for nine batches of 4096 acquisitions (repetition time [TR] = 1 s; total time 1 h 9 min) as the peak height divided by the root mean square of the noise after applying two times zero filling and 15 Hz line broadening. To determine the differences in $T_2{}^*$ between the different field strengths, the linewidth of the Glyc resonance was determined by taking the full width at half maximum in these processed spectra and subtracting the 15 Hz line broadening. The NOE factor was determined in two animals at each field strength by also acquiring a similar batch with the NOE turned off and dividing the Glyc C1 peak integral of the batch with NOE by that of the batch without NOE.

To assess the T_1 of brain and equivalent (8,17) muscle glycogen, an unlocalized inversion recovery pulse sequence consisting of an 8 ms adiabatic inversion pulse and an adiabatic excitation pulse was applied (in $n = 2$ animals at each magnetic field strength). The inversion time (TI) was varied in 11 steps from 1 ms to 7 s. The T_1 relaxation time was determined by fitting the signal intensity S with the three-parameter equation $S(TI) = S_{ss}(1 - \beta\exp(TI/T_1))$ in OriginPro (OriginLab Corp, Northampton, MA). Here S_{ss} is the steady state signal and β is a correction factor for taking incomplete inversion into account.

The rat was then replaced with a phantom containing 5 mM [1-^{13}C] Glc and 500 mM oyster Glyc (Sigma-Aldrich, St. Louis, MO) to calculate their absolute concentrations as described previously (9,10). Briefly, the three peaks of interest (Glyc C1 as well as the α and β conformation of Glc C1) were fitted through deconvolution with a gaussian curve using built-in scanner software (Agilent Technologies, Santa Clara, CA) to determine their signal intensity S. The Glyc C1 signal and the sum of the Glc C1α and C1β integrals were then used to determine the total brain Glyc and Glc concentrations, as follows:

$$[G]_{iv} = \frac{S_{G,iv}}{S_{G,ph}} \frac{S_{FA,iv}}{S_{FA,ph}} \alpha \frac{IE_{G,ph}}{IE_{G,iv}} [G]_{ph}, \qquad [1]$$

where G is Glc or Glyc, iv stands for in vivo, ph stands for phantom, FA is the formic acid reference bulb (used to correct for differences in coil loading), and $\alpha = 0.98$ is a factor to compensate for differences in T_1 and NOE between rat brain and oyster glycogen (equal to 1 for Glc). The resulting Glyc time courses were subjected to a standard Fisher F-test to determine if the hypothesis that the slope was zero could be rejected (18). This was accomplished from a linear fit of the time course and determining if $a/\sigma_a > qt_{0.05,7}$, where a is the slope of the linear fit, σ_a the standard deviation of this slope, and $qt_{0.05,7} = 1.895$ the 95% confidence quantile of the Student's t-test for the used number of degrees of freedom.

RESULTS

To account for the differences in quality between the radiofrequency coils used at the different magnetic field

Table 1
Results of the Glyc and Glc C1 Resonance Measurements at 9.4 and 14.1 T

Substance	B_0 (T)	lw (Hz)	SNR	T_1 (ms)	IE (%)	Concentration (mM)
Glyc	9.4	48 ± 8	7.4 ± 1.8	332 ± 15	39 ± 5	5.8 ± 0.9
	14.1	53 ± 9	12.3 ± 0.8	521 ± 34	36 ± 4	6.0 ± 0.4
Glc	9.4		16.4 ± 2.5	1930 ± 140		4.3 ± 0.4
	14.1		23.8 ± 2.4	2020 ± 180		4.4 ± 0.3

All errors are standard deviations of the mean of all animals at a field strength ($n = 4$ at 9.4 T and $n = 3$ at 14.1 T).

strengths, their loaded Q factors were determined on a network analyzer. At 14.1 T, $Q = 67 \pm 3$, while at 9.4 T $Q = 63 \pm 3$. The ratio of these loaded Q factors, which might have an influence on the SNR ratio between the two magnetic field strengths, was therefore 1.06. The noise figures of the 9.4 and 14.1 T scanners were 1.31 and 1.23 dB, respectively, resulting in a noise amplification of 1.16 and 1.15 and thus a factor 0.99 influence on the SNR ratio.

To enhance the ^{13}C NMR signal, the animals were prelabeled at the Glyc C1 position. The IE of Glyc C1 as determined from the IE of NAA was similar at both field strengths (39 ± 5% for $n = 4$ animals at 9.4 T and 36 ± 4% for $n = 3$ animals at 14.1 T, see Table 1). During the subsequent series of localized MR measurements (1 h 9 min per time point), the Glyc C1 resonance was consistently detected with high SNR of 6–14 (Fig. 1). The linewidths of the Glyc C1 resonance after shimming were similar and consistent at both field strengths (48 ± 8 Hz at 9.4 T and 53 ± 9 Hz at 14.1 T). As the inverse of these linewidths divided by π, the T_2^* relaxation times, there-

FIG. 1. A comparison of the spectra obtained at 9.4 T (upper spectrum) and 14.1 T (lower spectrum) in a volume of interest of 480 μL with TR = 1 and 1 h 9 min acquisition time (4096 repetitions). 15 Hz gaussian line broadening and two times zero filling have been applied, while for display the spectra are equalized to the height of the Glc C1β peak. Note the relatively narrow linewidth at 14.1 T, which leaves a wider baseline between the peaks.

fore, were estimated at 6.6 ± 1.1 and 5.9 ± 1.0 ms at 9.4 and 14.1 T, respectively. For the convenience of discussing the SNR differences found in the study, the relative SNR, rSNR = $SNR_{14.1\ T}/SNR_{9.4\ T}$ is introduced here; for Glyc C1, rSNR = ∼1.7 versus ∼1.5 for Glc C1β (Table 1), while the distance of the coil from the top of the rat head was the same within 0.5 mm and the same volume of interest (480 μL) was used. The Glyc C1 NOE amplification factor was 2.8 ± 0.1 at both field strengths.

The increased SNR together with the increased spectral dispersion and similar linewidths thus resulted in a more defined spectral baseline at 14.1 T: the resonances, including Glyc, were narrower (in ppm) and thus a wider and relatively flatter baseline between the resonances was apparent (Fig. 1). This allowed for more robust spectral peak fitting, which in turn allowed for a more accurate quantification through Eq. 1, as evidenced in the halving of the error of the calculated concentration of Glyc at 14.1 T compared to 9.4 T. The quantified brain Glyc time courses clearly demonstrate this improved quantification (Fig. 2): under the same physiological and equipment conditions, the Glyc time courses of the individual animals at 9.4 T as measured with the SIRENE sequence (Fig. 2a) have a visibly higher spread than those at 14.1 T (Fig. 2b).

The F-tests to determine the significance of the slope of the time courses at both magnetic field strengths resulted in ratios a/σ_a of the slope of the linear fit and its standard deviation that ranged from 0.08 to 1.04. These were all lower than the quantile $qt_{0.05,7} = 1.895$, which signified that the hypothesis that the slope was zero could not be rejected. This then meant that no significant increase or decrease of the glycogen concentration over time could be detected within the individual animals and that the individual time courses could be taken as constant over time. When all the measurements in all the animals at a magnetic field strength were then taken together, the standard deviation at 14.1 T was less than half than that at 9.4 T (Fig. 2c): $[Glyc]_{9.4\ T} = 5.8 \pm 0.9$ mM and $[Glyc]_{14.1\ T} = 6.0 \pm 0.4$ mM. Furthermore, a two-tailed Student's t-test ($\alpha = 0.05$) resulted in a $p = 0.38$ probability such that the means at 9.4 and 14.1 T were equal.

To determine the Glyc C1 T_1 relaxation time, an unlocalized adiabatic inversion recovery experiment was used. Fitting the exponential recovery curves was highly consistent and accurate: $R^2 = 0.998$ on average in $n = 2$ animals at both field strengths (Fig. 3). The TR and TI were chosen long enough to allow full relaxation at the longer TIs, while the adiabatic nature of the pulses allowed for an almost complete inversion of the magnetization at short TIs despite using a surface coil. The resulting T_1s of 332 ± 15 and 521 ± 34 ms demonstrate

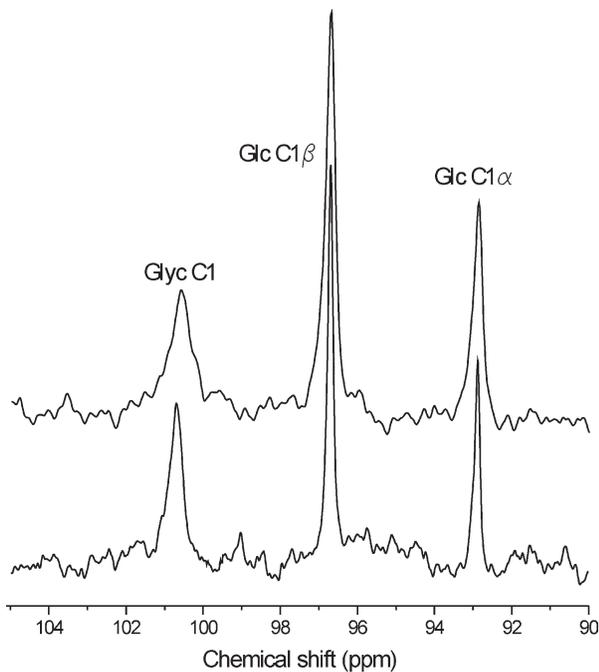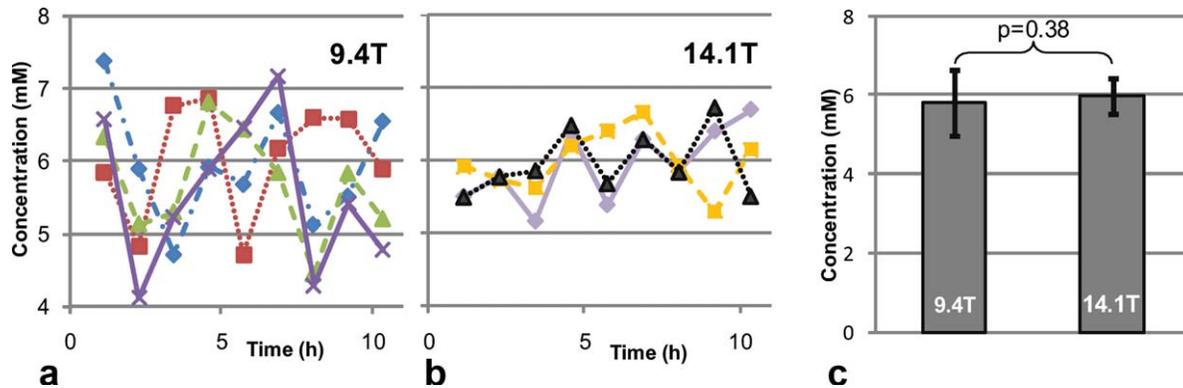FIG. 2. Overview of the spread of the glycogen concentration quantification. **a**: Time courses of the quantified glycogen of the individual animals ($n = 4$) at 9.4 T. Each time point represents 4096 localized ^{13}C acquisitions with TR = 1 s in a 480-µL volume of interest in one animal. **b**: Similar time courses for the rats ($n = 3$) at 14.1 T with the same volume of interest and number of scans. An overall smaller spread of the points can be observed compared to those at 9.4 T. **c**: Mean and standard deviation of all the individual points of quantified glycogen concentration in (a) and (b). The P value was calculated through a two-tailed Student's t-test with $\alpha = 0.05$.

an increase in T_1, resulting in a 10% decrease in rSNR when using a TR of 1 s (11).

DISCUSSION

The Glyc concentrations at both 9.4 and 14.1 T were consistent with literature (2,9,10). However, at 6.0 ± 0.4 mM the time course at 14.1 T had a significantly lower standard deviation than the 5.8 ± 0.9 mM at 9.4 T. The
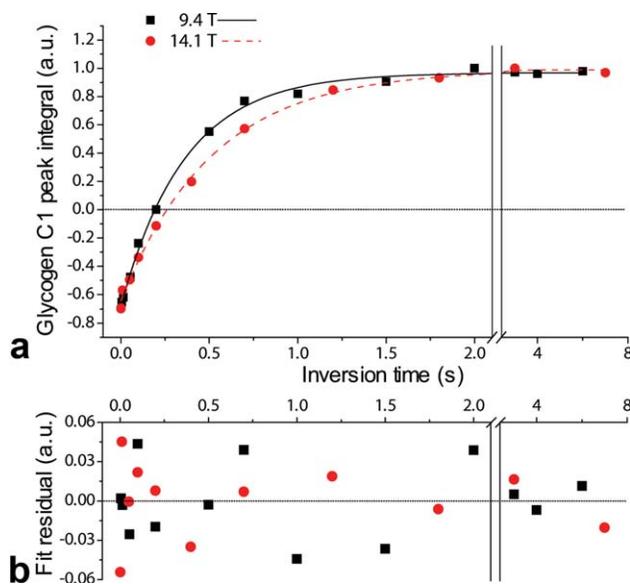

FIG. 3. Unlocalized glycogen inversion recovery curves at both field strengths illustrate the difference in T_1 relaxation time. The sequence had a sufficiently long TR (of 5 s) and sufficiently adiabatic excitation to allow full relaxation and near-full inversion. **a**: The fits were highly accurate ($R^2 = 0.998$ for both curves) and resulted in $T_1 = 332 \pm 15$ ms at 9.4 T (solid line) and $T_1 = 521 \pm 34$ ms at 14.1 T (dashed line). To better illustrate the different recovery times, completely recovered signal after a 2.0 s TI is displayed at a smaller scale. **b**: Residuals of the fits show a homogeneous spread, indicating that they mainly consist of noise. [Color figure can be viewed in the online issue, which is available at wileyonlinelibrary.com.]

factors that could contribute to the quantification process will therefore be discussed in the following paragraphs.

We have demonstrated that the prelabeling method for Glyc labeling is consistent at different magnet field strengths and results in readily quantifiable Glyc C1 resonances at both 9.4 and 14.1 T (39 ± 5 and $36 \pm 4\%$, respectively), indicating a consistent labeling to the degree that was observed in previous studies. If this nonsignificant difference is taken as an influence on the observed rSNR (rSNR$_{obs}$), a correction factor $39/36 = 1.08$ should be added to obtain the rSNR originating purely from differences in polarization at the two field strengths (rSNR$_{true}$). Similarly, rSNR$_{true}$ needs to be multiplied by $1.15/1.16 = 0.99$ to correct for the differences in noise figures of the receive chains.

The ratio of the loaded Q factors of the coils used at 14.1 and 9.4 T was 1.06. As SNR $\sim Q^{0.5}$, the rSNR$_{obs}$ overestimated the rSNR$_{true}$ detection by a factor 1.03.

The linewidth (and thus the estimated T_2^*) of Glyc also did not change significantly with the field increase, as expected through the field-indifferent T_2 and similar shimming. The NOE amplification at both field strengths was the same within experimental error and therefore did not contribute to the rSNR.

The calculated T_1 relaxation time increased proportionally with the magnetic field strength, consistent with literature (8,11). However, this increase in relaxation time also implies a relative decrease in rSNR. At the TR of 1 s, the equation for saturation recovery ($S = S_{ss}[1 - \exp(-TR/T_1)]$) results in 95% of signal recovery for $T_1 = 330$ ms, while 85% of the signal recovers when $T_1 = 520$ ms. The increased T_1 together with the relatively short TR, therefore, mean that the rSNR$_{obs}$ underestimated rSNR$_{true}$ by a factor 1.11 due to the incomplete recovery of the longitudinal magnetization.

With the factors above taken into account, the rSNR$_{true}$ $= 1.66 \times 1.11 \times 1.08 \times 0.99/1.03 = 1.91$, while a factor 1.5 would be expected purely from the magnetic field strength increase (19). However, it is the rSNR$_{obs}$ that plays a role in the quantification, indicating that the better definition of the baseline at 14.1 T may also contribute to the 2-fold decrease in standard deviation at 14.1

T. An increased SNR resulted in better baseline definition, while the increased spectral dispersion resulted in a larger range for definition of the baseline. The thus improved overall baseline characterization in concert with the increased SNR of the resonances likely allowed a more accurate gaussian peak fitting of the resonances. This peak fitting then was consistent in all animals and showed pure-noise residuals.

The Fisher *F*-test demonstrated that all individual Glyc time courses were constant over time, as expected since the animal physiology was kept constant throughout the experiments. Analogously, as anticipated through similar physiology and experimental protocols, the Student's *t*-test at $P = 0.38$ between the studies at 9.4 and 14.1 T showed no significant difference in the means of the concentrations.

In conclusion, to our best knowledge, this is the first report of in vivo ^{13}C-detected MR spectroscopy of brain glycogen at a field strength higher than 9.4 T. While the brain glycogen concentration was kept equal and constant at both magnetic field strengths, a clear increase in SNR and a more dispersed spectrum at 14.1 T offered a significant increase in quantification accuracy, despite the increase in T_1 relaxation times.

REFERENCES

1. Gruetter R. Glycogen: the forgotten cerebral energy store. J Neurosci Res 2003;74:179–183.
2. Morgenthaler FD, Koski DM, Kraftsik R, Henry PG, Gruetter R. Biochemical quantification of total brain glycogen concentration in rats under different glycemic states. Neurochem Int 2006;48:616–622.
3. Gibbs ME, Anderson DG, Hertz L. Inhibition of glycogenolysis in astrocytes interrupts memory consolidation in young chickens. Glia 2006;54:214–222.
4. Brown AM, Sickmann HM, Fosgerau K, Lund TM, Schousboe A, Waagepetersen HS, Ransom BR. Astrocyte glycogen metabolism is required for neural activity during aglycemia or intense stimulation in mouse white matter. J Neurosci Res 2005;79:74–80.
5. Petit JM, Tobler I, Kopp C, Morgenthaler F, Borbely AA, Magistretti PJ. Metabolic response of the cerebral cortex following gentle sleep deprivation and modafinil administration. Sleep 2010;33:901–908.
6. de Almeida Souza A, Seixas da Silva GS, Veleza BS, Menezes Santoroa AB, Montero-Lomelí M. Glycogen synthesis in brain and astrocytes is inhibited by chronic lithium treatment Neuroscience Lett 2010;482:128–132.
7. Oz G, Henry PG, Seaquist ER, Gruetter R. Direct, noninvasive measurement of brain glycogen metabolism in humans. Neurochem Int 2003;43:323–329.
8. Choi IY, Tkac I, Ugurbil K, Gruetter R. Noninvasive measurements of [1-(13)C]glycogen concentrations and metabolism in rat brain in vivo. J Neurochem 1999;73:1300–1308.
9. Morgenthaler FD, van Heeswijk RB, Xin L, Laus S, Frenkel H, Lei H, Gruetter R. Non-invasive quantification of brain glycogen absolute concentration. J Neurochem 2008;107:1414–1423.
10. van Heeswijk RB, Morgenthaler FD, Xin L, Gruetter R. Quantification of brain glycogen concentration and turnover through localized 13C NMR of both the C1 and C6 resonances. NMR Biomed 2010;23:270–276.
11. Overloop K, Vanstapel F, Van Hecke P. 13C-NMR relaxation in glycogen. Magn Reson Med 1996;36:45–51.
12. Adriany G, Gruetter R. A half-volume coil for efficient proton decoupling in humans at 4 Tesla. J Magn Reson 1997;125:178–184.
13. Hill HDW, Richards RE. Limits of measurement in magnetic resonance. J Phys E-Sci Instrum 1968;1:977–983.
14. Gruetter R. Automatic, localized in vivo adjustment of all first- and second-order shim coils. Magn Reson Med 1993;29:804–811.
15. Choi IY, Tkac I, Gruetter R. Single-shot, three-dimensional non-echo localization method for in vivo NMR spectroscopy. Magn Reson Med 2000;44:387–394.
16. Ordidge RJ, Connelly A, Lohman JAB. Image-selected in vivo spectroscopy (ISIS)—a new technique for spatially selective Nmr-spectroscopy. J Magn Reson 1986;66:283–294.
17. Chee NP, Geddes R, Wills PR. Metabolic heterogeneity in rabbit brain glycogen. Biochim Biophys Acta 1983;756:9–12.
18. Box GEP. Non-normality and tests on variances. Biometrika 1953;40:318–335.
19. Redpath TW. Signal-to-noise ratio in MRI. Br J Radiol 1998;71:704–707.